

Aldol Additions of Dihydroxyacetone Phosphate to *N*-Cbz-Amino Aldehydes Catalyzed by L-Fucose-1-Phosphate Aldolase in Emulsion Systems: Inversion of Stereoselectivity as a Function of the Acceptor Aldehyde

Laia Espelt,^[a] Jordi Bujons,^[a] Teodor Parella,^[b] Jordi Calveras,^[a] Jesús Joglar,^[a] Antonio Delgado,^[c, d] and Pere Clapés^{*[a]}

Abstract: The potential of L-fucose-1-phosphate aldolase (FucA) as a catalyst for the asymmetric aldol addition of dihydroxyacetone phosphate (DHAP) to *N*-protected amino aldehydes has been investigated. First, the reaction was studied in both emulsion systems and conventional dimethylformamide (DMF)/H₂O (1:4 v/v) mixtures. At 100 mM DHAP, compared with the reactions in the DMF/H₂O (1:4) mixture, the use of emulsion systems led to two- to three-fold improvements in the conversions of the FucA-catalyzed reactions. The *N*-protected aminopolyols thus obtained were converted to iminocyclitols by reductive amination with Pd/C. This reaction was highly diastereoselective with the exception of the reaction of the aldol adduct formed

from (*S*)-*N*-Cbz-alaninal, which gave a 55:45 mixture of both epimers. From the stereochemical analysis of the resulting iminocyclitols, it was concluded that the stereoselectivity of the FucA-catalyzed reaction depended upon the structure of the *N*-Cbz-amino aldehyde acceptor. Whereas the enzymatic aldol reaction with both enantiomers of *N*-Cbz-alaninal exclusively gave the expected 3*R*,4*R* configuration, the stereochemistry at the C-4 position of the major aldol adducts produced in the reactions with *N*-Cbz-glycinal and *N*-

Cbz-3-aminopropanal was inverted to the 3*R*,4*S* configuration. The study of the FucA-catalyzed addition of DHAP to phenylacetaldehyde and benzyloxycetaldehyde revealed that the 4*R* product was kinetically favored, but rapidly disappeared in favor of the 4*S* diastereoisomer. Computational models were generated for the situations before and after C–C bond formation in the active site of FucA. Moreover, the lowest-energy conformations of each pair of the resulting epimeric adducts were determined. The data show that the products with a 3*R*,4*S* configuration were thermodynamically more stable and, therefore, the major products formed, in agreement with the experimental results.

Keywords: biotransformations • DHAP-dependent aldolases • enzyme catalysis • iminocyclitols • lyases

Introduction

Stereoselective C–C bond formation catalyzed by aldolases has recently attracted tremendous interest as a powerful tool in asymmetric synthesis.^[1,2] Aldolases catalyze aldol additions of aldehydes and ketones with fine control of the absolute configuration of the newly formed stereogenic centers. In particular, dihydroxyacetone phosphate (DHAP) dependent aldolases^[3,4] catalyze the aldol addition of DHAP to a variety of non-natural aldehyde acceptors to generate two stereogenic centers and add three carbon atoms to the carbon backbone.^[5] Aldolases react highly stereoselectively at the C-3 position of DHAP (i.e., the stereocenter arising from DHAP addition), whereas the stereoselectivity at the C-4 position (i.e., the one generated from the addition to

[a] Dr. L. Espelt, Dr. J. Bujons, J. Calveras, Dr. J. Joglar, Dr. P. Clapés
Institute for Chemical & Environmental Research-CSIC
Jordi Girona 18–26, 08034-Barcelona (Spain)
Fax: (+34) 93-204-5904
E-mail: pcsqbp@iiqab.csic.es

[b] Dr. T. Parella
Servei de Ressonància Magnètica Nuclear Universitat Autònoma de Barcelona (Spain)

[c] Dr. A. Delgado
Unit of Medicinal Chemistry, Associated Unit to CSIC Faculty of Pharmacy, University of Barcelona (Spain)

[d] Dr. A. Delgado
RUBAM Institute for Chemical & Environmental Research-CSIC (Spain)

Supporting information for this article is available on the WWW under <http://www.chemeurj.org/> or from the author.

the aldehyde) depends on the structure and stereochemistry of the acceptor aldehyde (**1–4**, see Scheme 1).^[3,6,7]

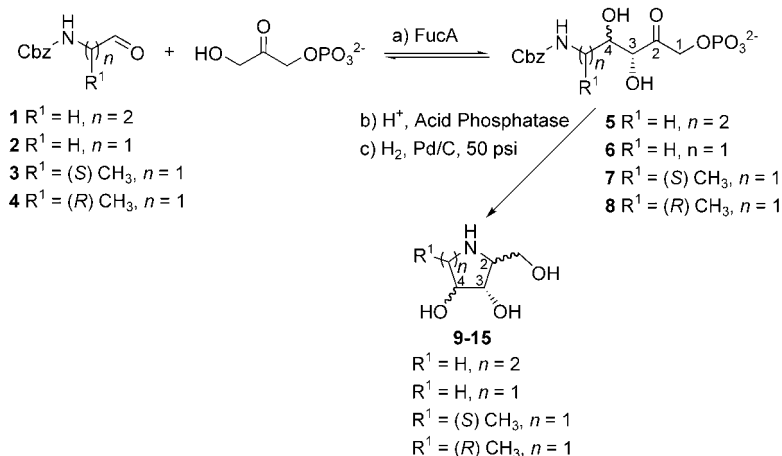
The stereoselective synthesis of aminopolyols and iminocyclitols using DHAP aldolases is currently a topic of interest in our laboratory. The key step in our strategy involves the aldol addition of DHAP to *N*-benzyloxycarbonyl (Cbz) amino aldehydes.^[7] We recently reported the use of D-fructose-1,6-diphosphate aldolase from rabbit muscle (RAMA) and L-rhamnulose-1-phosphate aldolase from *E. coli* (RhuA) as catalysts for this reaction. As a continuation of our research project, herein we report on the reactivity and stereoselectivity of recombinant L-fuculose-1-phosphate aldolase from *E. coli* (FucA)^[8] in the aldol reaction of *N*-Cbz-amino aldehydes^[7] **1–4** with DHAP (Scheme 1). In this study we focused on three aspects. Firstly, to assess whether the advantages of emulsion systems, already found to be useful in RAMA- and RhuA-catalyzed aldol reactions, applied to the new enzyme, the influence of the reaction medium on the conversion was systematically investigated. Secondly, to determine the stereoselectivity of FucA towards the acceptor aldehydes, the structure and stereochemistry of the resulting cyclic products, namely iminocyclitols, were analyzed. Thirdly, to understand the stereochemical outcome of the FucA-catalyzed aldol addition reactions, computational modeling of the aldehyde–DHAP–FucA complexes was carried out as well as conformational searches for each pair of possible epimeric products at C-4.

Results and Discussion

Influence of the reaction medium:

L-Fuculose-1-phosphate aldolase-catalyzed aldol additions of DHAP to aldehydes **1–4** (Scheme 1) were performed in both emulsion and DMF/water (1:4) cosolvent systems.^[7,9] Two DHAP concentrations, 45 and 100 mM with 1.8 equiv mol^{−1} of *N*-Cbz amino aldehyde, were examined. The data, given as a molar percentage of conversion, were the maximum values obtained and remained constant up to 12–24 h, even after the addition of more enzyme. Therefore it may be assumed that these conversions were close to the equi-

ilibrium values. As shown in Table 1, the aldehydes **1–4** are suitable acceptors for FucA aldolase, the degree of conversion to aldol adducts depending mainly on the reaction medium used. At 100 mM DHAP, better results were obtained with the emulsion systems than with the DMF/water mixtures (Table 1, entries 1, 3, 4, and 6), although under these conditions, aldehydes **1** and **3** only gave moderate conversions in the emulsion systems (Table 1, entries 1 and 4). Interestingly, lowering the DHAP concentration (45 mM) greatly improved the reaction conversions in DMF/H₂O (1:4), as well as for aldehydes **1** and **3** regardless of the reaction medium used (Table 1, entries 2, 5, and 7). Note that at high substrate concentrations, low conversions were also observed with fructose-1,6-diphosphate aldolase from rabbit muscle (RAMA) in DMF/H₂O (1:4) systems.^[7] This behavior appeared to be related to both the limited solubility of the acceptor aldehyde and the low stability of the enzyme in the reaction medium. Moreover, the improved conversion at the lower DHAP concentration also suggests that the aldolase is inhibited by the *N*-protected amino aldehyde^[6,10] or



Scheme 1. Chemo-enzymatic synthesis of linear *N*-Cbz-aminopolyols **5–8** (disodium salts) and iminocyclitols **9–15** from *N*-Cbz-amino aldehydes **1–4**. For the stereochemistry at C-4 of compounds **5–8**, see text. For the stereochemistry at C-2, C-4, and C-5 of compounds **9–15**, see Table 3.

Table 1. FucA-catalyzed aldol reaction between DHAP and *N*-Cbz-amino aldehydes.

Entry	Acceptor aldehyde	FucA [U mL ^{−1}]	DHAP [mM] ^[a]	Conversion [%] ^[b] (Time [h]) Reaction media ^[c]				Product
				A	B	C	D	
1	1	8	100	35 (8)	34 (6)	34 (5)	16 (4)	5
2	1	6	45	52 (6)	50 (6)	51 (6)	42 (6)	5
3	2	8	100	53 (8)	66 (5)	49 (5)	15 (4)	6
4	3	8	100	30 (7)	32 (7)	35 (7)	16 (1)	7
5	3	6	45	57 (2)	57 (5)	57 (3)	58 (5)	7
6	4	8	100	41 (8)	56 (4)	58 (3)	17 (4)	8
7	4	6	45	58 (7)	56 (7)	63 (7)	50 (4)	8

[a] Molar percent conversion to the aldol adduct (**5–8**) with respect to the starting DHAP concentration, determined by HPLC from the crude reaction mixture using purified standards. [b] Reaction conditions: A: H₂O/C₁₄E₄/tetradecane 90:4:6 wt %; B: H₂O/C₁₄E₄/hexadecane 90:4:6 wt %; C: H₂O/C₁₄E₄/squalane 90:4:6 wt %, where C₁₄E₄ is tetra(ethylene glycol) tetradecyl ether, C₁₄H₂₉(OCH₂CH₂)₄OH, with an average of 4 moles of ethylene oxide per surfactant molecule; D: DMF/H₂O (1:4 v/v). [c] 1.8 equiv mol^{−1} of acceptor aldehyde; reaction volume 5 mL, *T* = 25 °C.

by the methylglyoxal which results from DHAP decomposition.^[3]

Like L-rhamnulose-1-phosphate aldolase,^[7] FucA showed no clear preference for either of the two enantiomers of *N*-Cbz-alaninal (Table 1, entries 5 and 7), although at 100 mM DHAP the conversion to the *R* enantiomer was higher than the conversion to the *S* enantiomer (Table 1, entries 4 and 6). In contrast, high kinetic enantio-discrimination by FucA has been reported for a series of racemic 2-hydroxyaldehyde acceptors.^[11] These differences may be explained by the fact that 2-hydroxyaldehydes have a higher affinity and better orientation in the biocatalyst active site than the aldehydes **3** and **4** which have a hydrophobic methyl group.

Stereochemical characterization: Compounds **5–8** were synthesized (ca. 50–160 mg) and transformed into iminocyclitols by a previously described procedure (Scheme 1).^[7,12] The relative stereochemistries of the newly formed stereogenic centers of the iminocyclitols were unequivocally ascertained by one- and two-dimensional NMR techniques.^[13] This allowed us to quantify the diastereoisomers thus formed and to elucidate the stereoselectivity of FucA in the aldol addition of DHAP to aldehydes **1–4**. For the DHAP-aldolase catalysis, it is accepted that the absolute configuration at the C-3 position (i.e. *R* for FucA) (Scheme 1) is conserved upon reaction with electrophiles.^[14–19] Thus, the identified cyclic products and the absolute configuration of their stereogenic centers could be assessed (Table 2).

Similar to the NMR study on the iminocyclitols obtained with RAMA and RhuA aldolases,^[7] and as a complement to NOE data, the shielding effects were also used as a probe to assign the relative stereochemistry of **9–15** (Table 3). The OH(3) and CH₂OH(2) groups induced a 0.08–0.26 ppm upfield shift on the H-2 and H-3 protons of compound **13**, with respect to **14** and **15**, whereas a downfield shift was observed for the C-2, C-3, and C-4 carbon centers of **13** (Table 3). Moreover, when the OH(4) and Me(5) groups adopted a *cis* configuration (e.g. compounds **13** and **14**), a strong upfield ¹³C chemical shift of 3.2–3.5 ppm was induced on the Me(5) group. Similarly, a *cis* orientation of the CH₂OH(2) and OH(4) moieties caused an upfield ¹³C chemical shift on the C-4 carbon atom.

Inspection of the stereochemistry at the C-2 position revealed that the reductive amination of compounds **5**, **6**, and **8** with Pd/C was stereoselective, the hydrogen atom being

Table 2. Structures of the iminocyclitols derived from linear compounds **5–8**.

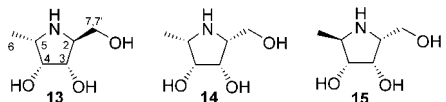
$\begin{array}{c} \text{1) Acid phosphatase} \\ \text{5.3 U mmol}^{-1} \text{ substrate} \\ \text{2) H}_2 \text{ 50 psi Pd/C, 24 h} \end{array} \quad \begin{array}{c} \text{5-8} \\ \longrightarrow \\ \text{9-15} \end{array}$				
Entry	Linear product/ [α] _D ²⁰ (c = 1 in MeOH)	Cyclic products	d.r.	Cyclic product or mixture [α] _D ²⁰
1	5/−8.9		76:24	−6.4 (c = 0.9 in MeOH)
2	6/−1.2		80:20	−21.2 (c = 0.8 in MeOH)
3	7/+1.0		55:45	−7.1 (c = 1.2 in MeOH)
4	8/+4.5		100:0	+37.9 (c = 1.4 in MeOH)

[a] See ref. [7]. [b] See refs. [20,21]. [c] Not previously described. [d] See refs. [22,23].

delivered from the face opposite the hydroxy group at the C-4 position.^[7] This was not found in the reductive amination of compound **7**; here, there was no face selectivity and about 50 % epimerization at C-2 was obtained.

Analysis of the stereochemistry at the C-4 position of the iminocyclitols **9–15** (Table 2) by high-field ¹H NMR spectroscopy allowed us to deduce, within the limits of detection, the stereoselectivity of FucA towards each of the *N*-Cbz-protected amino aldehydes. As Table 2 entries 1 and 2 shows, the major cyclic diastereoisomer obtained from aldehydes **1** and **2** (i.e. iminocyclitols **9** and **11**, respectively) has an *S* configuration at the C-4 position. This stereochemistry arose from attack of the enzyme–DHAP-enediolate complex on the *re* face of the carbonyl group of the aldehyde. Interestingly, this diastereofacial selectivity was the inverse of that found for the natural acceptor, L-lactaldehyde, and other non-natural aldehydes.^[24–26] In these cases, the DHAP–FucA complex attacks the carbonyl component at the *si* face, although the formation of diastereoisomers (3–30 %), epimeric at the C-4 position, has been reported.^[14] On the other hand, FucA was highly stereoselective towards both enantiomers of Cbz-alaninal with approximately 99 % *de* of the expected 4*R* diastereoisomer (iminocyclitols **13–15**) being formed.

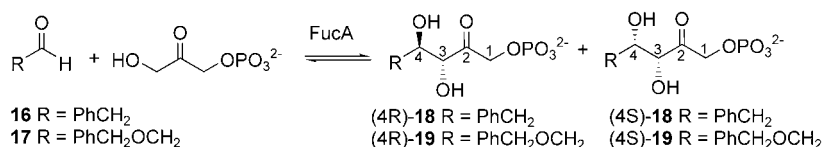
We then asked if the stereochemical outcome of FucA-catalyzed aldol addition reactions was kinetically or thermodynamically controlled. Stereochemical analysis of the adducts formed at the beginning of the reaction and after long incubation times may shed light on this point. RP-HPLC was experimentally the most convenient method for this purpose, however, the diastereoisomers of the aldol prod-

Table 3. ^1H and ^{13}C chemical shifts [ppm] of the iminocyclitols **13**, **14**, and **15**.


Product	$\delta(\text{H/C})2$	$\delta(\text{H/C})3$	$\delta(\text{H/C})4$	$\delta(\text{H/C})5$	$\delta(\text{H/C})6$	$\delta(\text{H/C})7$	$\delta(\text{H/C})7'$
13	3.51/62.1	4.19/71.7	4.22/78.3	3.65/57.2	1.30/11.8	3.87/58.7	3.76/58.7
14	3.69/58.4	4.45/70.4	4.10/71.5	3.61/56.9	1.32/11.5	3.79/58.6	3.73/58.6
15	3.75/61.5	4.27/70.4	3.95/76.7	3.54/56.7	1.38/15.0	3.92/58.4	3.80/58.4

ucts formed from the reactions of the amino aldehydes **1–4** could not be resolved by this technique. Interestingly, the inversion of stereoselectivity induced by FucA in these reactions was also observed in the aldol addition reactions of

respective of their orientation of attack (*si* or *re*), which are stabilized by a hydrogen bond between their carbonyl oxygen atom and the phenol group of Tyr113'. A model for the binding of L-lactaldehyde to DHAP-complexed FucA

Scheme 2. FucA-catalyzed aldol addition of DHAP to phenylacetaldehyde (**16**) and to benzyloxyacetaldehyde (**17**).

both phenylacetaldehyde (**16**) and benzyloxyacetaldehyde (**17**) (Scheme 2). In these cases, the diastereoisomers obtained could be resolved by RP-HPLC and quantified.^[27] Hence it was thought that these reactions may be helpful in the analysis of the stereochemical course of the reaction and most of the studies that follow were carried out with these substrates. The progress of the aldol addition reaction, as depicted in Figure 1, revealed that both (4R)-**18** and (4R)-**19** were kinetically favored while their epimers, (4S)-**18** and (4S)-**19**, respectively, were the major products obtained and, presumably, thermodynamically more stable (approximate ratio 70:30). Note that the rate of formation of the 4S products was quite fast, being the major adducts after 50–60 min.

Computational models: To gain an insight into the mechanisms responsible for the above observations, computational models pertinent to both enzyme–substrate and enzyme–product complexes were generated and conformational analysis of the aldol products was performed.

Computational models were generated for the reaction intermediates before and after C–C bond formation between DHAP and aldehydes **16** and **17** in the active center of FucA (I and II, respectively, in Scheme 3), as previously reported for other aldolases.^[7,26] The starting point for these models was the reported crystal structure of wild-type FucA with the inhibitor phosphoglycolohydroxamate (PGH) bound to its active site.^[28] This structure lacks the coordinates of the mobile C-terminal tail of the protein (residues 207–215), which has been proposed to undergo an induced fit upon substrate binding (vide infra).^[26]

has been proposed in which the high stereoselectivity of the enzyme was attributed mainly to analogous interactions between the carbonyl and hydroxy groups of the substrate and the phenol group of Tyr113'.^[26] At variance with this L-lactaldehyde binding model, the absence of an α -hydroxy group in aldehydes **16** and **17** favors an orientation in which their aromatic substituents are directed towards the hydrophobic wall formed by the side chains of Phe131 and Phe206'. Similar interactions were observed in the corresponding models for adducts **18** and **19** (see Supporting Information). However, the conformational differences due to the two possible orientations of attack (*si* or *re*) of the aldehydes or between the two corresponding epimeric adducts are rather small. Therefore, it seems plausible that the differences between the geometries and, by extension, the energies of the corresponding transition states should be small. This could explain the relatively small kinetic preference shown by the enzyme in the reactions with aldehydes **16** and **17**.

As stated above, the mobile C-terminal tail of the protein was initially omitted from these simulations because of the lack of structural data. Joerger et al.^[26] proposed a model for the induced fit of this tail suggesting that, upon substrate binding, it undergoes a conformational shift from a less-ordered state to one in which it covers the entrance to the active center of FucA. This allowed some of its residues (i.e. Tyr209') to come into contact with the substrates, thus rendering a more packed structure around the active site. Therefore, we performed further docking simulations that included the coordinates of the modeled C-terminal tail of the protein.^[30] The results obtained for aldehydes **16** and **17** are shown in panels C and D of Figure 2, while those for the corresponding adducts **18** and **19** can be found in the Supporting Information.

As could be anticipated, the aldehydes that are larger than the natural substrate, L-lactaldehyde, could sterically

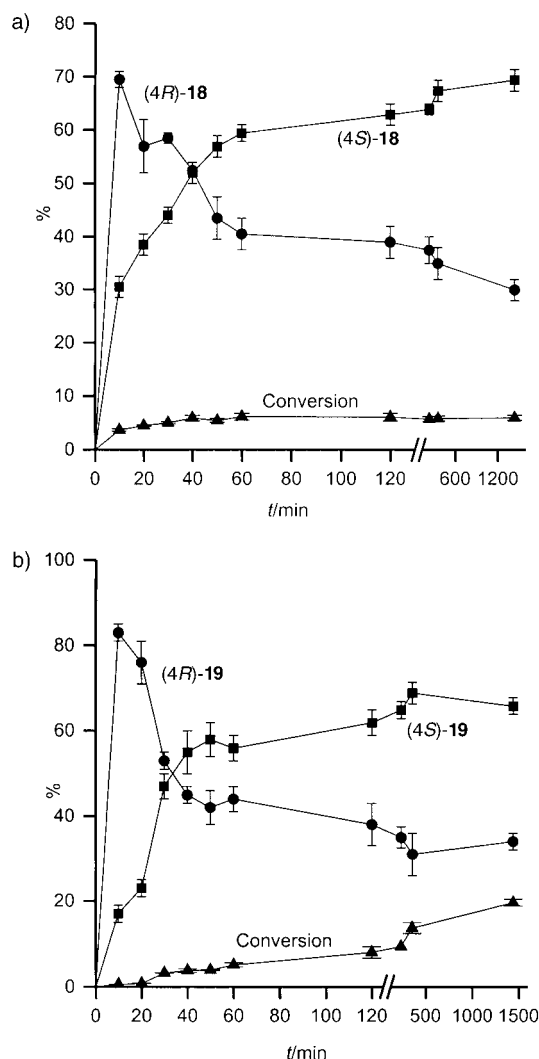
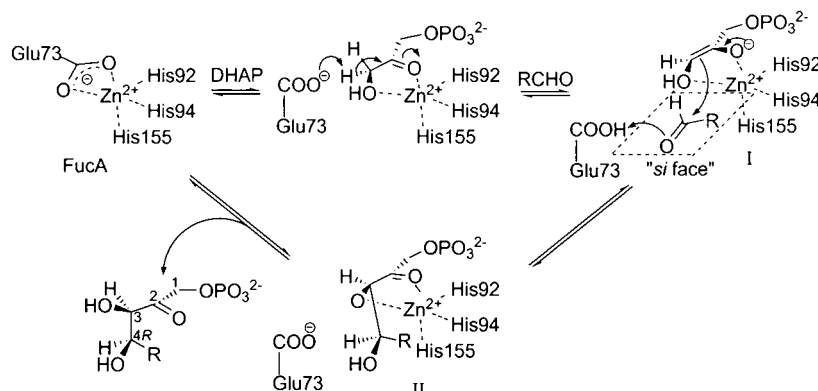


Figure 1. Time-course of the FucA-catalyzed aldol reaction between DHAP and a) phenylacetaldehyde **16** and b) benzyloxyacetaldehyde **17**. Relative molar percentages of (4*R*)-**18**, (4*S*)-**18**, (4*R*)-**19** and (4*S*)-**19** formation and molar percentage conversion with respect to the starting DHAP concentration. Reactions were carried out in H₂O/C₁₄E₄/hexadecane (90:4:6 wt %) emulsion systems: [DHAP]=30 mM, 1.8 equiv mol⁻¹ of **16** or **17**, and 1–2.5 U mL⁻¹ FucA; reaction volume=2.5 mL and *T*=25 °C.



Scheme 3. Proposed enzymatic mechanism for the FucA-catalyzed aldol addition reactions.^[26,29] The stereochemistry at the C-4 position of the adducts is determined by the face (*si* or *re*) of the aldehyde that approaches the reactive C-3 atom of the DHAP-enediolate.

interfere with the proposed conformation of the C-terminal fragment of the protein. Consequently, the resulting minimized conformations of **16** and **17** are directed away from the Phe131 and Phe206' residues and towards the inner part of the enzyme pocket. Again, only small differences could be observed between the conformations derived from the *si* or *re* approach of the carbonyl group to the enediolate, and also between the minimized conformations obtained for the epimers of products **18** and **19**. These models provided no evidence for stabilizing interactions between the substrates and Tyr209' but, since the simulations were carried out with a fixed protein structure, it cannot be ruled out that they would be established if the structure of the protein was allowed to relax. However, it seems reasonable to think, as mentioned earlier, that the size of these substrates could pose a significant steric hindrance that would hamper, or even prevent, the induced fit of the C-terminal FucA tail. This would lead to a reduction in the activity of the enzyme and a modified stereoselectivity towards the aldehyde, both of which were observed with the substrates used in this study. Hence, the reduced, but not zero, activities reported for different C-terminus FucA mutants suggest that this tail is not essential for enzyme activity.^[26] In addition, these mutants gave higher proportions of the *L-threo* adducts derived from the "wrong" *re* approach of the aldehyde molecule to the DHAP-enediolate.

The time course of the reaction of aldehydes **16** and **17** shown in Figure 1 indicated a thermodynamic control of the reaction products. To substantiate this assumption, we performed an extensive exploration of the conformational space of each of the C-4 epimers of adducts **18** and **19**, and this was extended to **5–8**. We considered only the linear forms of these products since our NMR data indicate that the relative abundance of the corresponding cyclic forms always accounted for between 5 and 50% of the total adducts present in the crude reaction products. To this end, we first ran a systematic conformational search on every molecule (see Experimental Section). The energies were calculated by using the Merck force field (MMFF94)^[31] and the Born continuum solvation model,^[32–34] which have been successfully used in the modeling of polar compounds^[35] and carbohydrates.^[36,37]

Table 4 summarizes the calculated energetic differences between the lowest energy conformations found for each pair of epimers, while the corresponding geometries and actual energy values are reported in the Supporting Information. Table 4 also shows both the experimental and predicted ratios of the 4*R* and 4*S* adducts; the latter were calculated from the energy differences mentioned above, assuming that the entropic contributions to ΔG

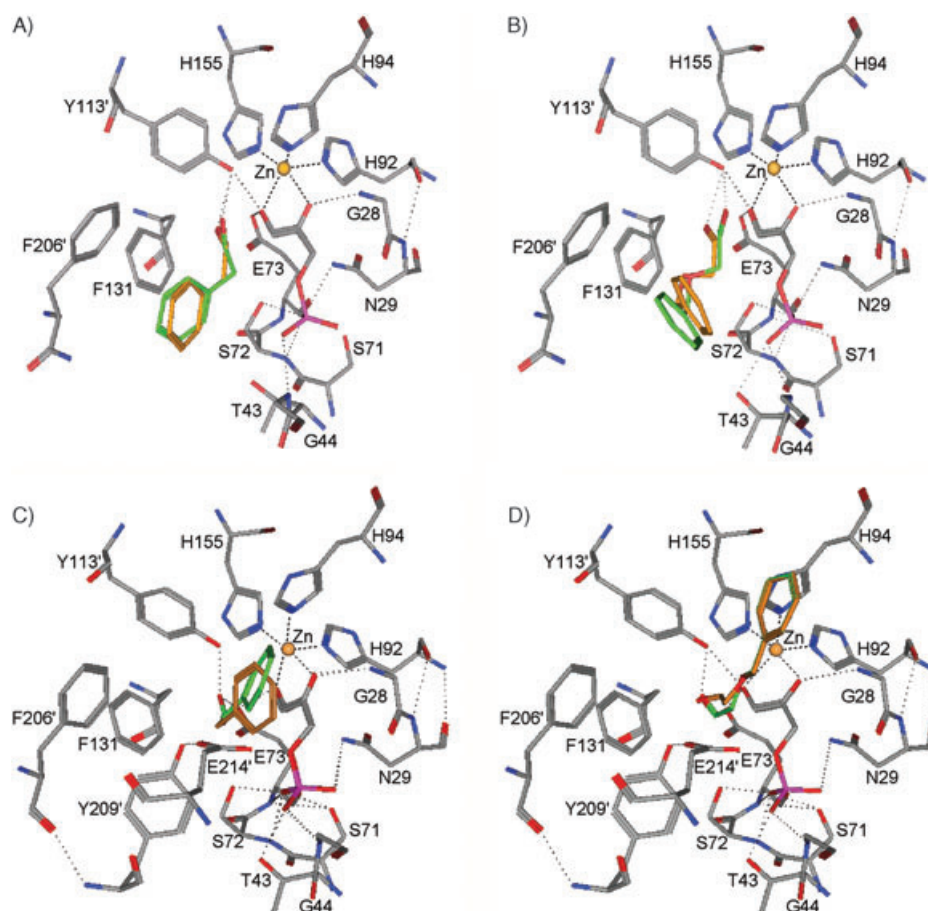


Figure 2. Structural models of aldehydes **16** (panels A and C) and **17** (panels B and D) in the active center of FucA, approaching the Zn^{2+} -bound DHAP-enediolate from their *si* (green) and *re* (orange) faces. Panels A and B: Models generated from the reported crystallographic coordinates of FucA.^[28] Panels C and D: Models generated from a modeled FucA structure that includes coordinates of the proposed induced fit of the mobile C-terminal tail.^[26]

Table 4. Energy differences (ΔE^{4R-4S}) between the global minima determined for the 4*R* and 4*S* epimers of the aldol adducts **5–8**, **18**, and **19**, and the predicted and experimental compositions of the reaction mixtures.

Product	ΔE^{4R-4S} [kcal mol ⁻¹]	Ratio 4 <i>R</i> :4 <i>S</i> (predicted)	Ratio 4 <i>R</i> :4 <i>S</i> (experimental)
5	1.1	13:87	24:76
6	0.4	33:67	20:80
7	−0.6	73:27	~100:0
8	−1.0	84:16	~100:0
18	0.4	33:67	30:70
19	0.9	18:82	30:70

should be similar. It is clear that there is a good correlation between the predicted and experimental values for products **5–8**, **18**, and **19**. Thus, the global minima determined for the 4*S* epimers of adducts **5**, **6**, **18**, and **19** have lower energies than the corresponding minima determined for the 4*R* epimers and, accordingly, these are the major reaction products, while the opposite is true for the diastereoisomers of adducts **7** and **8**.

The experimental and computational results collected in this work for the formation of aldol adducts **18** and **19** suggest the reaction coordinate scheme depicted in Figure 3 is operative. This is similar to the one proposed for *N*-acetylneuraminic acid aldolase.^[38] Hence, aldehydes **16** and **17** could approach the FucA-bound DHAP-enediolate by either of the two possible reactive orientations, with the *si* approach energetically preferred over the *re* approach. However, the energetically preferred reaction products are those derived from the attack of the enediolate on the *re* face of the carbonyl group and therefore these are the major products of the reaction. This hypothesis may be extended to the rest of the *N*-Cbz-amino aldehydes considered in this study since they have analogous steric hindrance. To verify this hypothesis additional quantum mechanics/molecular mechanics (QM/MM) modeling studies are being carried out in order to accurately calculate the energy barriers of these reaction coordinates.

Conclusions

L-Fucose-1-phosphate aldolase catalyzed the aldol addition of DHAP to several *N*-Cbz-amino aldehydes in conversion yields that range from 50 to 60 %. At 100 mM DHAP the emulsion systems gave the highest substrate conversion to aldol adduct compared with those achieved in DMF/H₂O (1:4) mixtures. Together with earlier findings,^[7] the high-water-content emulsions appear to be of general applicability, yet easy to prepare, for DHAP-aldolase-catalyzed aldol addition reactions, especially when dealing with low-water-soluble aldehyde acceptors.

We report here an inversion of stereoselectivity in FucA-catalyzed aldol addition of DHAP to *N*-Cbz-glycinal, *N*-Cbz-3-aminopropanal, phenylacetaldehyde, and benzyloxycetaldehyde. Time-progress curves for the reactions with phenylacetaldehyde and benzyloxycetaldehyde revealed that the products with the “natural” 4*R* configuration were kinetically favored, whereas the inverted 4*S* ones were the major products formed, which suggests that the reactions have a thermodynamic outcome. Computational models of

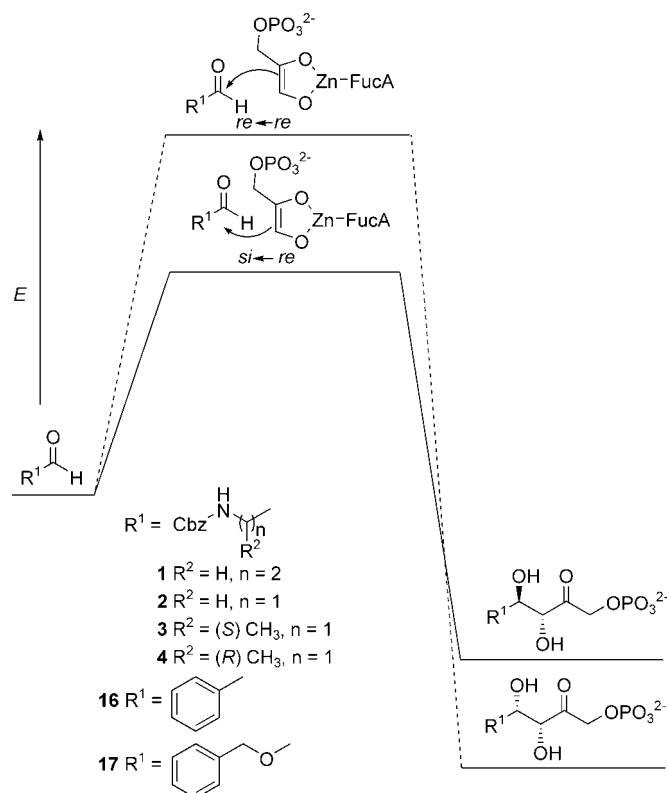


Figure 3. Proposed reaction coordinate for the FucA-catalyzed aldol addition to the aldehydes considered in this study.

substrates and products complexed to the active-site cavity of the enzyme and theoretical calculations of the energy differences between the lowest-energy conformers of each pair of aldol epimers at C-4 substantiate the above experimental results.

Experimental Section

Materials: L-Fucose-1-phosphate aldolase was produced at the Departament d'Enginyeria Química, Universitat Autònoma de Barcelona, from recombinant *E. coli* (ATCC no 86984) and purified by affinity chromatography. Acid phosphatase (PA, EC 3.1.3.2, 5.3 U mg⁻¹) was from Sigma (St. Louis, USA). The non-ionic poly(oxyethylene ether) surfactant, tetra(ethylene glycol) tetradecyl ether, C₁₄H₂₉(OCH₂CH₂)₄OH (C₁₄E₄), with an average of 4 mol of ethylene oxide per surfactant molecule (C₁₄E₄), was from Albright & Wilson (Barcelona, Spain). Tetradecane (99%), hexadecane (99%), and 2,6,10,15,19,23-hexamethyltetracosane (squalane) (99%) were from Sigma. DOWEX (H⁺) 50×8 ion-exchange resin was from Fluka. HPLC isocratic grade acetonitrile was from Merck (Darmstadt, Germany) and Multisolvant acetonitrile for preparative RP-HPLC was from Scharlau (Barcelona, Spain). MacroPrep High Q Support anion-exchange resin was from BioRad (Hercules, USA). Triethylamine (Calbiochem, San Diego, USA) was of buffer grade. Phenylacetaldehyde and benzyloxycetaldehyde were from Aldrich (Milwaukee, USA). N-Benzyloxycarbonyl amino aldehydes **1–4** were synthesized in our laboratory by using previously described procedures.^[7] The precursor of dihydroxyacetone phosphate (DHAP), dihydroxyacetone phosphate dimer bis(ethyl ketal), was synthesized in our laboratory by using a procedure similar to that described by Jung et al.^[39] De-ionized water was

used for preparative HPLC and Milli-Q grade water for both analytical HPLC and gel-emulsion formation. All other solvents and chemicals used in this work were of analytical grade.

Methods: Molecular modeling: All molecular simulations were conducted with the MOE program (v. 2003.02, Chemical Computing Group, Montreal) using the MMFF94 force field with its standard atomic charges and parameters.^[31] All energy calculations were carried out by using the Born continuum solvation model^[32–34] as implemented in the MOE program. For the FucA complexes, a smoothed cut-off between 14 and 15 Å was used to model the nonbonded interactions. All minimizations were performed up to an RMS gradient of <0.01.

The coordinates for *E. coli* fucose-1-phosphate aldolase complexed to phosphoglycolohydroxamate (PGH)^[28] were obtained from the Protein Data Bank^[40] at Brookhaven National Laboratory (entry 4FUA). The structure includes the coordinates of one FucA monomer with the essential Zn²⁺ ion complexed to PGH, one molecule of β-mercaptoethanol covalently bound to Cys14, one sulfate anion, and several water molecules. Nine C-terminal residues (residues 207–215) were missing from the crystal structure, and therefore they were not initially included in the original simulations although they were considered at a later stage (see text). By applying the necessary crystallographic symmetry operators to this structure, the homotetramer that constitutes the biological unit was built. Since the active center of FucA is located at the interface between each pair of contiguous monomers, each homotetramer contains four catalytic centers. However, in order to reduce the calculation time, the simulations were performed on a FucA dimer that contained just one catalytic site. In addition, the sulfate and the solvent molecules were removed, the hydrogen atoms were added, and the PGH molecule was conveniently modified to obtain the α-hydroxyketonic adducts **18** and **19** complexed to the Zn²⁺ cation in the catalytic active center (state II of Scheme 3). The conformational space of these ligands was explored to find the low-energy minima by running a stochastic conformational search keeping the coordinates of the protein and the essential Zn²⁺ fixed.

The structure of the ligands was further modified to generate the situation before the C–C bond formation, as represented by state I in Scheme 3, in which the aldehyde molecule is close to the Zn²⁺-coordinated DHAP-enediolate. To avoid the exclusion of this aldehyde molecule, a restraint was imposed between the two carbon atoms that participate in the C–C bond formation (i.e., the C-3 atom of the enediolate and the C-1 atom of the aldehyde). This restraint was arbitrarily set so as to keep the distance between these two carbon atoms close to 2.5 Å to ensure that both substrates would adopt conformations that resemble those of the putative transition states. The conformational space of the aldehydes was then stochastically searched as before, keeping the coordinates of the rest of the atoms fixed.

The conformational spaces of compounds **5–8**, **18**, and **19** were exhaustively searched by using the two different strategies available in the MOE program in order to find the global energy minima. First, starting from an initially optimized structure, a systematic conformational search was run in which every non-amide nonterminal single bond was rotated in 60–120° steps. The conformations generated for each compound, which in some cases amounted to several hundred thousands, were then minimized and ranked according to their energy. To confirm the nature of the lowest energy conformer determined, a subsequent stochastic conformational search was run using a procedure similar to that reported by Auzanneau et al.^[36] Briefly, the conformational space of the molecules was explored by random rotation of bonds and simultaneous Cartesian perturbation. The conformations thus generated were minimized and checked to determine, within an RMS tolerance (0.1 Å), whether they were duplicates of previously generated conformations. The process was terminated when the number of failures to find new conformations exceeded a large enough number (1000) of consecutive attempts.

HPLC analyses: HPLC analyses were performed on a Lichograph[®] HPLC system (Merck, Darmstadt, Germany) fitted with a RP-HPLC cartridge, 250×4 mm, filled with Lichrosphere[®] 100, RP-18, 5 μm (Merck). Samples (50 mg) were withdrawn from the reaction medium, dissolved in methanol (0.5–1 mL) to stop any enzymatic reaction, and subsequently analyzed by HPLC. The solvent systems used were: solvent A: 0.1 % v/v

trifluoroacetic acid (TFA) in H₂O; solvent B: 0.095% v/v TFA in H₂O/CH₃CN (1:4), gradient elution from 10 to 70% B in 30 min, flow rate 1 mL min⁻¹, UV detection 215 nm. The retention factors (*k'*) for each aldol condensation product are given below.

NMR analysis: High-field ¹H and ¹³C NMR analyses of the compounds under study in D₂O solutions were carried out at the Servei de Resonància Magnètica Nuclear, Universitat Autònoma de Barcelona, using an AVANCE 500 BRUKER spectrometer. The compounds were fully characterized by typical gradient-enhanced 2D experiments, COSY, NOESY, HSQC, and HMBC, under routine conditions. When possible, NOE data was obtained from selective 1D NOESY experiments by using a single pulsed-field-gradient echo as a selective excitation method and a mixing time of 500 ms. When necessary, proton and NOESY experiments were recorded at different temperatures to study the different behavior of the exchange phenomena and thereby avoiding the presence of false NOE cross-peaks that make both structural and dynamic studies difficult. ¹H (300 MHz) and ¹³C NMR (75 MHz) spectra of compounds in [D₆]DMSO and D₂O solutions were recorded with a Varian Unity-300 spectrometer at the Instituto de Investigaciones Químicas y Ambientales-CSIC.

Elemental analyses and specific rotations: Elemental analyses were performed by the Servei de Microanàlisi Elemental IQAB-CSIC. Specific rotations were measured with a Perkin Elmer Model 341 (Überlingen, Germany) polarimeter.

Enzymatic aldol condensations in emulsions (conditions A, B, and C, Table 1): The emulsion systems consisted of ternary mixtures of water (90 wt%), technical grade tetra(ethylene glycol) tetradecyl ether surfactant, C₁₄H₂₉(OCH₂CH₂)₄OH (C₁₄E₄) (4 wt%), with an average of 4 mol of ethylene oxide per surfactant molecule, and either tetradecane (C₁₄), hexadecane (C₁₆), or squalane (C₃₀) (6 wt%). The reactions were carried out in 10 mL screw-capped test-tubes. The aldehyde (0.4–0.9 mmol), oil (6% w/w), and the surfactant (4% w/w) were mixed vigorously. The DHAP solution (0.225–0.500 mmol) at pH 6.9, freshly prepared as described by Effenberger and Straub,^[41] was then added dropwise to the surfactant mixture while stirring at 25 °C with a vortex mixer. The final reaction volume was 5 mL. Finally, FucA (6–8 U mL⁻¹) was added and the solution mixed again. The test-tubes were placed in a horizontal shaking bath (100 rpm) maintained at a constant temperature (25 °C). The reactions were followed by HPLC until the peak of the product reached a maximum. The enzymatic reactions were stopped by addition of MeOH and the final crude mixture purified as described previously.^[7]

Enzymatic aldol condensations in mixtures of dimethylformamide/water (1:4) (condition D, Table 1): The reactions were carried out in 10-mL screw-capped test-tubes. The aldehyde (0.4–0.9 mmol) was dissolved in DMF (1 mL). Then, the DHAP solution (4 mL, 0.225–0.500 mmol), prepared as described above, was added dropwise while mixing. The rest of the experimental procedure was identical to that described above for the reaction in emulsions.

Physical data for the linear compounds 5–8: The melting points of the compounds given below correspond to lyophilized solids rather than crystals. Note that some of them are mixtures of C-4 epimers. The yields correspond to the amounts of product derived from the aldol enzymatic reactions at the semipreparative level. The purification procedures were not optimized.

(3R,6-(Benzyloxycarbonylamino)-5,6-dideoxy-1-O-phosphonohex-2-ulose disodium salt (5): The title compound (160 mg, 35% yield) was prepared by using conditions A (see Table 1) with 45 mM DHAP. HPLC: *k'* = 5.2; m.p. 109–111 °C (99.9% pure by HPLC); elemental analysis calcd (%) for C₁₄H₁₈NO₉Na₂P·H₂O·NaCl: C 33.79, H 4.05, N 2.81; found: C 33.95, H 3.71, N 2.60. The ¹H and ¹³C NMR spectra of the product, a mixture of two diastereoisomers, were consistent with those previously reported.^[7]

(3R,5-(Benzyloxycarbonylamino)-5-deoxy-1-O-phosphonopent-2-ulose disodium salt (6): The title compound (130 mg, 26% yield) was prepared by using conditions B (see Table 1) with 100 mM DHAP. HPLC: *k'* = 4.1; m.p. 114–118 °C (99.9% pure by HPLC); elemental analysis calcd (%) for C₁₃H₁₆NO₉Na₂P·⁵/₂H₂O·NaCl: C 30.55, H 4.11, N 2.74; found: C 30.55, H 4.24, N 2.44. The ¹H and ¹³C NMR spectra of the product, a mix-

ture of two diastereoisomers along with cyclic species, were consistent with those previously reported.^[7]

(3R,5S)-5-(Benzyloxycarbonylamino)-5,6-dideoxy-1-O-phosphonohex-2-ulose disodium salt (7): The title compound (180 mg, 46% yield) was prepared by using conditions B (see Table 1) with 45 mM DHAP. HPLC: *k'* = 4.5; m.p. 113–115 °C (99.9% pure by HPLC); elemental analysis calcd (%) for C₁₄H₁₈NO₉Na₂P·¹/₂H₂O·NaCl: C 36.05, H 4.29, N 3.00; found: C 36.38, H 4.28, N 2.74.

(3S,5R)-5-(Benzyloxycarbonylamino)-5,6-dideoxy-1-O-phosphonohex-2-ulose disodium salt (8): The title compound (320 mg, 56% yield) was prepared by using conditions C (see Table 1) with 45 mM DHAP. HPLC: *k'* = 4.5; m.p. 119–123 °C (99.9% pure by HPLC); elemental analysis calcd (%) for C₁₄H₁₈NO₉Na₂P·⁵/₂H₂O: C 35.99, H 4.92, N 3.00; found: C 35.90, H 4.77, N 2.95.

Removal of the phosphate group and catalytic hydrogenation: The phosphate group of compounds 9–15 was removed by acid phosphatase catalyzed hydrolysis following the procedure described by Bednarski et al.^[42] The resulting products were hydrogenated with 50 psi H₂ in the presence of Pd/C for 24 h as previously described.^[7]

(2S,3S,4S)-2-(Hydroxymethyl)piperidine-3,4-diol (9) and (2R,3S,4R)-2-(hydroxymethyl)piperidine-3,4-diol (10): The title compounds were prepared according to the general procedure described above. The ¹H and ¹³C NMR spectra of the major 9 and minor 10 diols were consistent with those reported previously.^[7]

(2S,3S,4S)-2-(Hydroxymethyl)pyrrolidine-3,4-diol (11) and (2R,3S,4R)-2-(hydroxymethyl)pyrrolidine-3,4-diol (12): The title compounds were prepared according to the general procedure described above. The ¹H and ¹³C NMR spectra of the major 11 and minor 12 diols were consistent with those reported previously.^[7]

(2S,3S,4R,5S)-2-(Hydroxymethyl)-5-methylpyrrolidine-3,4-diol (13) and (2R,3S,4R,5S)-2-(hydroxymethyl)-5-methylpyrrolidine-3,4-diol (14): The title compounds were prepared according to the general procedure described above. ¹H NMR (500 MHz, D₂O, 25 °C) major product, 13: δ = 4.22 (dd, ³J(H,H) = 3.8, ³J(H,H) = 8.8 Hz, 1H; H4), 4.19 (t, ³J(H,H) = 3.2 Hz, 1H; H3), 3.87 (dd, ³J(H,H) = 3.9, ³J(H,H) = 12.3 Hz, 1H; H7), 3.76 (d, 1H; H7), 3.65 (m, 1H; H5), 3.51 (m, ³J(H,H) = 3.5 Hz, ³J(H,H) = 9.0 Hz, 1H; H2), 1.30 ppm (d, ³J(H,H) = 6.7 Hz, 3H; H6); minor product, 14: δ = 4.45 (dd, ³J(H,H) = 4.5, ³J(H,H) = 7 Hz, 1H; H3), 4.10 (dd, ³J(H,H) = 4.9, ³J(H,H) = 9 Hz, 1H; H4), 3.79 (dd, ³J(H,H) = 11.9 Hz, 1H; H7), 3.73 (dd, ³J(H,H) = 3.5, ³J(H,H) = 11.9 Hz, 1H; H7), 3.69 (m, 1H; H2), 3.61 (m, 1H; H5), 1.32 ppm (d, ³J(H,H) = 6.7 Hz, 3H; H6); ¹³C NMR (125 MHz, D₂O, 25 °C) major product, 13: δ = 78.3 (C4), 71.3 (C3), 62.1 (C2), 58.1 (C7), 57.2 (C5), 11.8 ppm (C6); minor product 14: δ = 71.5 (C4), 70.4 (C3), 58.4 (C2), 58.6 (C7), 56.9 (C5), 11.5 ppm (C6).

(2R,3S,4R,5R)-2-(Hydroxymethyl)-5-methylpyrrolidine-3,4-diol (15): The title compound was prepared according to the general procedure described above. ¹H NMR (500 MHz, D₂O, 25 °C): δ = 4.27 (t, ³J(H,H) = 3.7 Hz, 1H; H3), 3.95 (dd, ³J(H,H) = 3.7 ³J(H,H) = 9 Hz, 1H; H4), 3.92 (dd, ³J(H,H) = 4.7, ³J(H,H) = 11.8 Hz, 1H; H7), 3.80 (dd, ³J(H,H) = 8.4 Hz, 1H; H7), 3.75 (m, ³J(H,H) = 3.7, ³J(H,H) = 4.7, ³J(H,H) = 8.4 Hz, 1H; H2), 3.54 (m, 1H; H5), 1.38 ppm (d, ³J(H,H) = 6.7 Hz, 3H; H6); ¹³C NMR (125 MHz, D₂O, 25 °C): δ = 76.7 (C4), 70.4 (C3), 61.5 (C2), 58.4 (C7), 56.7 (C5), 15.0 ppm (C6).

(3R,4S)-5-Deoxy-5-phenyl-1-O-phosphonopent-2-ulose disodium salt ((4S)-18): The title compound was prepared according to the general procedure described above. HPLC: *k'* = 3.2. ¹H NMR (300 MHz, D₂O, 25 °C): δ = 7.2 (m, 5H; Ph), 4.5 (dd, ³J(H,H) = 7.0 Hz, ³J(H,H) = 18.4 Hz, 2H; CH₂OP), 4.1 (m, 2H; 2(CHOH)), 2.7 ppm (m, 2H; CH₂Ph); ¹³C NMR (75 MHz, D₂O, 25 °C): δ = 213.7 (CO), 140.5 (C quat), 131.9 (C ar), 131.1 (C ar), 129.1 (C ar), 79.3 (CHOH), 75.1 (CHOH), 70.3 (CH₂OP), 41.1 ppm (CH₂).

(3R,4R)-5-Deoxy-5-phenyl-1-O-phosphonopent-2-ulose disodium salt ((4R)-18): The title compound was prepared according to the general procedure described above. HPLC: *k'* = 2.9. ¹H NMR (300 MHz, D₂O, 25 °C): δ = 7.2 (m, 5H; Ph), 4.5 (dd, ³J(H,H) = 6.0 Hz, ³J(H,H) = 18.7 Hz, 2H; CH₂OP), 4.3 (d, ³J(H,H) = 5.5 Hz, 1H; 2(CHOH)), 4.0 (m, ³J(H,H) = 4.0 Hz, ³J(H,H) = 5.1 Hz, ³J(H,H) = 5.5, 1H; CHOH), 2.8 ppm

(m, 2H; CH₂Ph); ¹³C NMR (75 MHz, D₂O, 25°C): δ=213.7 (CO), 140.5 (C quat), 131.9 (C ar), 131.1 (C ar), 129.1 (C ar), 79.8 (CHOH), 75.4 (CHOH), 71.0 (CH₂OP), 40.1 ppm (CH₂).

(3R,4S)-5-O-Benzyl-1-O-phosphonopent-2-ulose disodium salt ((4S)-19): The title compound was prepared according to the general procedure described above. HPLC: *k'*=4.6. ¹H NMR (300 MHz, D₂O, 25°C): δ=7.2 (m, 5H; Ph), 4.5 (m, 2H; CH₂OP), 4.4 (s, 2H; CH₂Ph), 4.3 (d, ³J(H,H)=1.8 Hz, 1H; CHOH), 4.1 (m, ³J(H,H)=2.2 Hz, ³J(H,H)=5.5 Hz, 1H; CHOH), 3.5 ppm (m, 2H; CH₂O); ¹³C NMR (75 MHz, D₂O, 25°C): δ=212.9 (CO), 139.5 (C quat), 131.1 (C ar), 130.9 (C ar), 130.7 (C ar), 78.1, 75.5, 72.6, 72.1, 70.6 ppm (CH and CH₂); ¹H NMR (300 MHz, [D₆]DMSO, 25°C): δ=7.2 (m, 5H; Ph), 4.8 (dd, ³J(H,H)=6.9, ³J(H,H)=18.3 Hz, 2H; CH₂OP), 4.5 (s, 2H; CH₂Ph), 4.1 (d, ³J(H,H)=1.8 Hz, 1H; CHOH), 3.9 ppm (dt, ³J(H,H)=6, ³J(H,H)=9.3 Hz, 1H; CH₂O); ¹³C NMR (75 MHz, [D₆]DMSO, 25°C): δ=207.8 (CO), 138.5 (C quat), 128.3 (C ar), 127.5 (C ar), 127.4 (C ar), 76.1, 72.2, 70.4, 70.3, 69.1 ppm (CH and CH₂).

(3R,4R)-5-O-Benzyl-1-O-phosphonopent-2-ulose disodium salt ((4R)-19): The title compound was prepared according to the general procedure described above. HPLC: *k'*=4.3. ¹H NMR (300 MHz, D₂O, 25°C): δ=7.2 (m, 5H; Ph), 4.5 (m, 2H; CH₂OP), 4.4 (s, 2H; CH₂Ph), 4.3 (d, ³J(H,H)=1.5 Hz, 1H; CHOH), 4.0 (m, ³J(H,H)=5.1 Hz, 1H; CHOH), 3.4 ppm (m, 2H; CH₂O); ¹³C NMR (75 MHz, D₂O, 25°C): δ=212.9 (CO), 139.5 (C quat), 131.1 (C ar), 130.9 (C ar), 130.7 (C ar), 78.1, 75.5, 72.7, 71.7, 71.0 ppm (CH and CH₂).

Acknowledgements

Financial support from the Spanish CICYT (PPQ2002-04625-CO2-01 and BQU2003-01677) is acknowledged. J.C. acknowledges the CSIC for the I3P predoctoral scholarship. We thank Prof. Josep López-Santín and the team at the Chemical Engineering Department, Universitat Autònoma de Barcelona, for the supply of FucA aldolase. The authors gratefully acknowledge Dr. G. E. Schulz and Dr. A. C. Joerger for providing the coordinates for the FucA model, which include the induced fit of the C-terminal tail.

- T. D. Machajewski, C.-H. Wong, *Angew. Chem.* **2000**, *112*, 1406–1430; *Angew. Chem. Int. Ed.* **2000**, *39*, 1353–1374.
- W.-D. Fessner, V. Helaine, *Curr. Opin. Biotechnol.* **2001**, *12*, 574–586.
- W.-D. Fessner, C. Walter, *Top. Curr. Chem.* **1996**, *184*, 97–194.
- H. J. M. Gijzen, L. Qiao, W. Fitz, C.-H. Wong, *Chem. Rev.* **1996**, *96*, 443–473.
- C.-H. Wong, R. L. Halcomb, Y. Ichikawa, T. Kajimoto, *Angew. Chem.* **1995**, *107*, 453–474; *Angew. Chem. Int. Ed. Engl.* **1995**, *34*, 412–432.
- R. Schoevaert, F. vanRantwijk, R. A. Sheldon, *J. Org. Chem.* **2001**, *66*, 4559–4562.
- L. Espelt, T. Parella, J. Bujons, C. Solans, J. Joglar, A. Delgado, P. Clapés, *Chem. Eur. J.* **2003**, *9*, 4887–4899.
- FucA was produced by the Department of Chemical Engineering, Universitat Autònoma de Barcelona, within the framework of a collaborative CYCIT project (PPQ2002-04625-CO2-01).
- L. Espelt, P. Clapés, J. Esquena, A. Manich, C. Solans, *Langmuir* **2003**, *19*, 1337–1346.
- R. L. Pederson, J. Esker, C.-H. Wong, *Tetrahedron* **1991**, *47*, 2643–2648.
- W.-D. Fessner, J. Badia, O. Eyrish, A. Schneider, G. Sinerius, *Tetrahedron Lett.* **1992**, *33*, 5231–5234.
- Iminocyclitols were obtained from compounds **5–8** in two steps (Scheme 1). Firstly, the phosphate group was removed by treatment with acid phosphatase followed by desalting by RP-HPLC. No baseline separation of the putative diastereoisomers was observed by analytical RP-HPLC. Therefore, the purpose of the purification step was to isolate the aldol adducts from the other species present in the reaction media. Secondly, both the deprotection of the amino group and the subsequent reductive amination were performed in a one-pot procedure by treatment with H₂ at 50 psi in the presence of 10% Pd/C. Aqueous solutions of each of the iminocyclitols in their free-base form were adjusted to pH 6.5, lyophilized, and submitted to NMR analysis without any further purification.
- In previous work (see ref. [7]), the relative configurations at the C-3 and C-4 positions of the linear structures **6–8** could not be unambiguously assigned by NMR analysis owing to overlapping signals resulting from the equilibria between the linear adducts and the corresponding cyclic hemiaminals. This was not the case with compound **5**; less than 5% of the hemiaminal was formed and the proportion of both diastereoisomers of the linear compound could be determined.
- W.-D. Fessner, G. Sinerius, A. Schneider, M. Dreyer, G. E. Schulz, J. Badia, J. Aguilar, *Angew. Chem.* **1991**, *103*, 596–599; *Angew. Chem. Int. Ed. Engl.* **1991**, *30*, 555–558.
- T. Gefflaut, C. Blonski, J. Perie, M. Willson, *Prog. Biophys. Mol. Biol.* **1995**, *63*, 301–340.
- W.-D. Fessner, A. Schneider, H. Held, G. Sinerius, C. Walter, M. Hixon, J. V. Schloss, *Angew. Chem.* **1996**, *108*, 2366–2369; *Angew. Chem. Int. Ed. Engl.* **1996**, *35*, 2219–2221.
- A. Dalby, Z. Dauter, J. A. Littlechild, *Protein Sci.* **1999**, *8*, 291–297.
- D. R. Hall, G. A. Leonard, C. D. Reed, C. I. Watt, A. Berry, W. N. Hunter, *J. Mol. Biol.* **1999**, *287*, 383–394.
- A. R. Plater, S. M. Zgiby, G. J. Thomson, S. Qamar, C. W. Wharton, A. Berry, *J. Mol. Biol.* **1999**, *285*, 843–855.
- C.-H. Wong, D. P. Dumas, Y. Ichikawa, K. Koseki, S. J. Danishefsky, B. W. Weston, J. B. Lowe, *J. Am. Chem. Soc.* **1992**, *114*, 7321–7322.
- Y. F. Wang, D. P. Dumas, C.-H. Wong, *Tetrahedron Lett.* **1993**, *34*, 403–406.
- T. Sifferlen, A. Defoin, J. Streith, D. Le Nouen, C. Tarnus, I. Dosbaa, M.-J. Foglietti, *Tetrahedron* **2000**, *56*, 971–978.
- A. Defoin, T. Sifferlen, J. Streith, I. Dosbaa, M.-J. Foglietti, *Tetrahedron: Asymmetry* **1997**, *8*, 363–366.
- C.-H. Wong, R. Alajarin, F. Moris-Varas, O. Blanco, E. Garcia-Junceda, *J. Org. Chem.* **1995**, *60*, 7360–7363.
- M. Mitchell, L. Qiao, C.-H. Wong, *Adv. Synth. Catal.* **2001**, *343*, 596–599.
- A. C. Joerger, C. Gosse, W.-D. Fessner, G. E. Schulz, *Biochemistry* **2000**, *39*, 6033–6041.
- The stereochemistry of each chromatographic peak was identified by applying NMR techniques to purified samples of the major diastereoisomers and to diastereomeric mixtures of the minor ones.
- M. K. Dreyer, G. E. Schulz, *J. Mol. Biol.* **1996**, *259*, 458–466.
- A. C. Joerger, C. Mueller-Dieckmann, G. E. Schulz, *J. Mol. Biol.* **2000**, *303*, 531–543.
- Kindly provided by G. E. Schulz and A. C. Joerger.
- T. A. Halgren, *J. Comput. Chem.* **1996**, *17*, 490–519.
- D. Qui, S. Shenkin, F. P. Hollinger, W. C. Still, *J. Phys. Chem. A* **1997**, *101*, 3005–3014.
- W. C. Still, A. Tempczyk, R. C. Hawley, T. Hendrickson, *J. Am. Chem. Soc.* **1990**, *112*, 6127–6129.
- M. Schaefer, M. Karplus, *J. Phys. Chem.* **1996**, *100*, 1578–1599.
- P. A. Nielsen, T. Liljefors, *J. Comput.-Aided Mol. Des.* **2001**, *15*, 753–763.
- F. I. Auzanneau, E. Sourial, J. M. Schmidt, M. Feher, *Can. J. Chem.* **2002**, *80*, 1088–1095.
- S. Perez, A. Imbert, S. B. Engelsen, J. Gruza, K. Mazeau, J. Jimenez-Barbero, A. Poveda, J. F. Espinosa, B. P. van Eyck, G. Johnson, A. D. French, M. Louise, C. E. Kowijzer, P. D. J. Grootenuis, A. Bernardi, L. Raimondi, H. Senderowitz, V. Durier, G. Vergoten, K. Rasmussen, *Carbohydr. Res.* **1998**, *314*, 141–155.
- W. Fitz, J.-R. Schwark, C.-H. Wong, *J. Org. Chem.* **1995**, *60*, 3663–3670.
- S.-H. Jung, J.-H. Jeong, P. Miller, C.-H. Wong, *J. Org. Chem.* **1994**, *59*, 7182–7184.

- [40] H. M. Berman, J. Westbrook, Z. Feng, G. Gilliland, T. N. Bhat, H. Weissig, I. N. Shindyalov, P. E. Bourne, *Nucleic Acids Res.* **2000**, 28, 235–242.
- [41] F. Effenberger, A. Straub, *Tetrahedron Lett.* **1987**, 28, 1641–1644.
- [42] M. D. Bednarski, E. S. Simon, N. Bischofberger, W.-D. Fessner, M. J. Kim, W. Lees, T. Saito, H. Waldmann, G. M. Whitesides, *J. Am. Chem. Soc.* **1989**, 111, 627–635.

Received: June 28, 2004
Published online: January 24, 2005